doi:10.1017/S1431927622002318
Microsc. Microanal. 28 (Suppl 1), 2022

Crystallization by Amorphous Particle Attachment and the Evolution of Texture in Biogenic Calcium Carbonate

Vanessa Schoeppler[1*], Deborah Stier[2], Benjamin H. Savitzky[3], Colin Ophus[3], Matthew A. Marcus[4], Karen C. Bustillo[3] and Igor Zlotnikov[2]

[1.] Department of Physics, University of California, Berkeley, USA.
[2.] B CUBE - Center for Molecular Bioengineering, Technische Universität Dresden, Dresden, Germany.
[3.] National Center for Electron Microscopy, Molecular Foundry, Lawrence Berkeley National Laboratory, Berkeley, CA, USA.
[4.] Advanced Light Source, Lawrence Berkeley National Laboratory, Berkeley, USA.
* Corresponding author: vschoeppler@lbl.gov

The study of the formation-structure-function-relationships of bio-composites has deepened our understanding of evolution driven materials engineering, and has provided biomimetic inspiration for their application. An important example is the biomineralization process of calcium carbonate through amorphous precursors that are morphed into shapes and textural patterns that cannot be produced by the classical monomer-by-monomer approach but instead crystallize by particle attachment (CPA). CPA is a gradual process where each step has its own thermodynamic and kinetic constraints defining a unique pathway of crystal growth [1,2].

In this work, researchers from TU Dresden, Germany, the National Center for Electron Microscopy (Lawrence Berkeley National Laboratory), and the Advanced Light Source (Lawrence Berkeley National Laboratory) made a fundamental leap in the ability to analytically describe the evolution of form and texture of biological mineralized tissues formed by CPA [3]. By utilizing EBSD, HRTEM, 4DSTEM and STXM analysis it was shown that texture development in the prisms of molluscan shells (Figure 1) is a spontaneous process dependent on the initial calcite lattice orientation of a prism with respect to the direction of growth; elastic energy is released during the amorphous calcium carbonate to calcite phase transformation through the formation of dislocations (Figure 2). These results provide not only key insight into material morphogenesis during crystallization by amorphous particle attachment but also teach us fundamental new mechanisms that have a profound effect on textural evolution during non-classical crystal growth. The analysis establishes a mechanistic link between the emergence of texture and the cumulative growth rate by amorphous particle accretion.

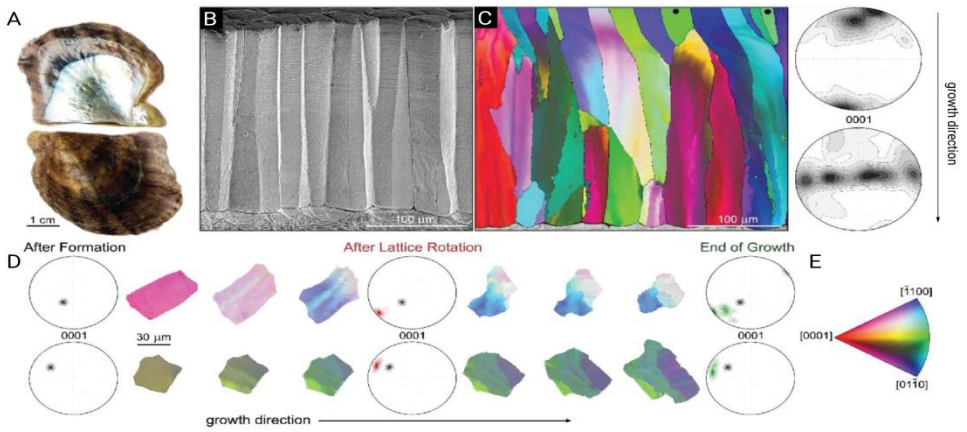

Figure 1. Textural evolution of the prismatic ultrastructure in the bivalve shell *Pinctada nigra*. A) The bivalve shell of P. nigra. B) Fracture of the prismatic architecture in *P. nigra* imaged parallel to the direction of growth. C) EBSD map of the prismatic architecture in *P. nigra* obtained parallel to the direction of growth. The corresponding color-coded inverse pole figure of calcite, with the reference direction normal to the image plane, is depicted in (E). Prisms that have their crystallographic c-axis of calcite parallel to the direction of growth and do not rotate are marked by black dots. (0001)-pole figures describe the overall texture of the prismatic assembly at the beginning and at the end of growth. D) A 3D-EBSD series of two prisms from *P. nigra* obtained perpendicular to the direction of growth taken with approximately 15 µm steps along the direction of growth. (0001)-pole figures describe the overall texture of the prisms at different stages of formation. E) Color-coded inverse pole figure of calcite, with the reference direction normal to the image plane.

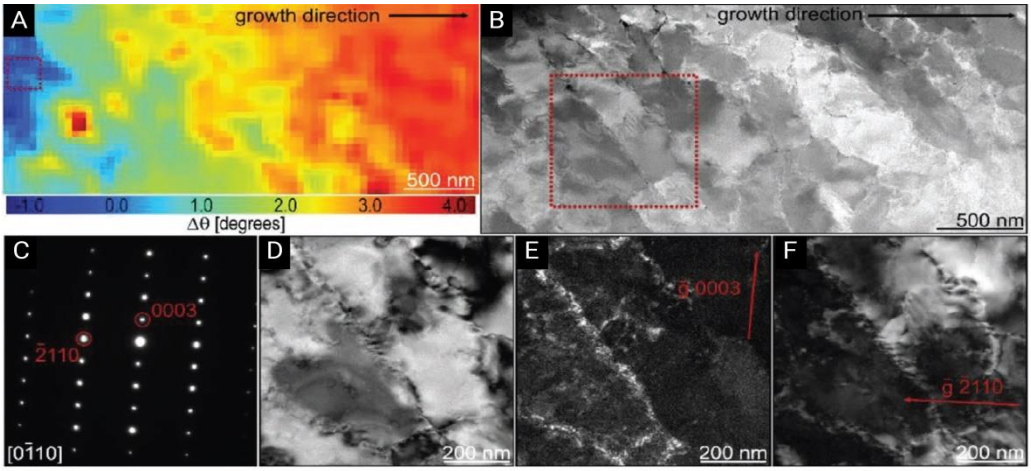

Figure 2. Dislocation analysis using transmission electron microscopy of a TEM lamella taken from the prisms of *P. nobilis.* A) Misorientation map displaying the change in lattice orientation in P. nigra relative to the area marked by a red rectangle obtained using 4D scanning electron nano-diffraction microscopy (4D-STEM) analysis. B) Scanning transmission electron microscopy (STEM) image of the TEM lamella investigated with 4D-STEM in (A). Red rectangle indicates the area further studied using the two-beam condition. C) Electron diffraction pattern of the area indicated in (B). D) Bright field image with g = 0003. E) Dark field image with g = 0003. F) Dark field image with g = 2110.

References:

[1] H. Cölfen, Crystals **10** (2020), p. 61. doi.org/10.3390/cryst10020061
[2] J. J. De Yoreo et al., Science **349** (2015), aaa6760-1 doi/10.1126/science.aaa6760
[3] V. Schoeppler et al., Advanced Materials **33** (2021), 2101358 doi.org/10.1002/adma.202101358

https://doi.org/10.1017/S1431927622002318 Published online by Cambridge University Press